

Supplement of Geosci. Model Dev., 11, 1909–1928, 2018  
<https://doi.org/10.5194/gmd-11-1909-2018-supplement>  
© Author(s) 2018. This work is distributed under  
the Creative Commons Attribution 4.0 License.



*Supplement of*

**Modeling soil CO<sub>2</sub> production and transport with dynamic source  
and diffusion terms: testing the steady-state assumption  
using DETECT v1.0**

**E. M. Ryan et al.**

*Correspondence to:* Edmund M. Ryan ([edmund.ryan@lancaster.ac.uk](mailto:edmund.ryan@lancaster.ac.uk))

The copyright of individual parts of the supplement might differ from the CC BY 4.0 License.

## Section S1 Description of how time- and depth-varying root biomass, soil organic matter, and microbial biomass carbon were estimated.

### Root Carbon

Root biomass carbon ( $C_R$ ) is expressed as the total amount of root biomass in a 1 m x 1 cm<sup>2</sup> column of soil ( $R^*$ ) times the fraction of roots at each depth  $z$ ,  $f_R(z)$ , scaled by an index of vegetation activity (greenness):

$$C_R(z, t) = R^* \cdot f_R(z) \cdot G(t)$$

where  $G(t) = \left(1 + \frac{\text{Greenness}(t) - \text{mean}(\text{Greenness})}{\text{max}(\text{Greenness}) - \text{min}(\text{Greenness})}\right)$  and *Greenness* is vegetation greenness, which was estimated every 2-4 weeks between March and September by taking digital photographs using a 2 m high camera stand and a 1 m<sup>2</sup> ground frame; images were analyzed following methods described by Zelikova *et al.* (2015), and linear interpolations were used to estimate *Greenness* on non-measurement dates. The scaling by *Greenness* via  $G(t)$  allows root C to vary over time ( $t$ ), where the rate of change of *Greenness* is assumed as being a proxy for the rate of change of root biomass C. The calculation of *Greenness* results in this quantity (scaling factor) varying between ~0.5 and ~1.5 because the depth-varying measurements of root C mass were made in the middle of the growing season. Our conservative estimation of the seasonal range of root biomass is based on a 3-fold difference in root production across the growing season as estimated from minirhizotron data (Carrillo *et al.*, 2014). The function  $R^* \cdot f_R(z)$  was estimated by fitting an exponential function,  $R^* \exp(-z/\lambda)$ , to site-level root biomass data collected at multiple depths (2.5, 10, 22.5, 37.5, 60, and 87.5 cm; Figure S4), where  $R^*$  and  $\lambda$  are parameters estimated via the fitting procedure.  $R^*$  represents the total amount of root C in the soil profile, while  $\lambda$  (estimate to be ~7) controls the slope of the curve (i.e., how fast root biomass declines with depth).

### Soil Carbon and Microbial Biomass Carbon

A similar approach was used to describe how soil organic matter (SOM) carbon ( $C_{SOM}$ ) and microbial biomass carbon ( $C_{MIC}$ ) vary with depth. The depth distribution of SOM is described as:

$$C_{SOM}(z) = S^* \cdot f_S(z)$$

where  $f_S(z)$  is an exponential decay function given by:  $f_S(z) = \exp(-z/\lambda)$ . We fit the exponential function to SOM data representing multiple depths (2.5, 10, 22.5 cm; Figure S4), giving an estimate of  $\lambda=30$ . A gamma distribution function was used to describe  $C_{MIC}$  such that:

$$C_{MIC}(z) = M^* \cdot f_M(z)$$

$f_M(z) = \text{gampdf}(z, a, b)$ , where *gampdf* is the gamma probability density function, as parameterized by Matlab. We fit the *gampdf* function to measurements of microbial biomass carbon also obtained for the same depths, leading to estimates of  $a = 1.7$  and  $b = 4.75$ . As with root carbon,  $S^*$  and  $M^*$  represent the total SOM and total microbial biomass carbon in a 1 m x 1 cm<sup>2</sup> soil column. We assumed that the  $C_{SOM}$  and  $C_{MIC}$  profiles were invariant with time for the single growing season that we simulated.

## Section S2 Calculation of initial conditions

The initial ( $t = 0$ ) CO<sub>2</sub> concentration for at each depth  $z$  was calculated in two stages:

(1) We used the following function:  $c(z, 0) = 356 + (Q \cdot C_{max} \cdot z) / (Q \cdot z + C_{max})$ , where  $C_{max}$  and  $Q$  are parameters that describe the curvature of the function, and  $z$  is the soil depth ( $0 \text{ m} \leq z \leq 1 \text{ m}$ ). By

informally fitting this equation to observations of soil CO<sub>2</sub> concentrations from the start of the 2007 growing season, taken from four different depths, we found that  $C_{max} = 4500$  and  $Q = 375$ . (2) We ran the DETECT model forward during the growing season of 2007, using the initial conditions (CO<sub>2</sub> concentrations at all depths for first day of model run) estimated from stage (1) (described above). The modelled soil CO<sub>2</sub> concentrations for all depths from the final day of the 2007 model run (September 31, 2007) was used as the initial conditions for the 2008 model runs that were used for the analysis of this study. See Figure S6 for the estimated versus observed CO<sub>2</sub> concentrations.

### Section S3 Mass balance equation checks for the DETECT and DETECT-SS models.

The mass balance of the DETECT and DETECT-SS models is theoretically guaranteed because equation 1 of the paper is actually the mass balance equation. The mass balance equation is defined as:

$$IN + PROD = OUT + ACC,$$

where for our model, IN and OUT are the inputs and outputs of CO<sub>2</sub> from the boxes below and above it in the soil profile, PROD is the production of CO<sub>2</sub>, and ACC is the accumulation of CO<sub>2</sub> over time. We can rearrange this mass balance equation to put it in the form of equation 1 from the manuscript:

$$ACC = (IN - OUT) + PROD$$

Where ACC is the  $dc/dt$  term from equation 1,  $(IN - OUT)$  is the  $d(Dgs*dC/dz)/dz$  term, and PROD is the S term. Similar comments can be made for the steady-state version of the DETECT model except that the ACC term in the above mass balance equation is equal to zero, i.e. there is no accumulation of soil CO<sub>2</sub> over time (or the  $dC/dt$  term in equation 1 is set to zero).

As a practical check, we created a Matlab script which computes the total {Rsoil + change in CO<sub>2</sub> storage} for both the DETECT and DETECT-SS models. Over the course of the year, {Rsoil + change in CO<sub>2</sub> storage} was 497.1 gC/m<sup>2</sup> for the DETECT model and 497.1 gC/m<sup>2</sup> for the DETECT-SS model, under the control scenario.

### Section S4 Alternative formulations of the functions that describe how soil CO<sub>2</sub> production changes with soil water content

To test the robustness of the DETECT model, we try alternative formulations of the function  $f$  that describe the production of soil CO<sub>2</sub> from root and microbial sources for different soil water content ( $\theta$ ) values. The formulation used in the paper (equation 4a) is an exponential function that depends on current and past soil water content. An alternative formulation is one where soil CO<sub>2</sub> production increases as  $\theta$  increases up to an optimum soil water content ( $\theta_{opt}$ ) value. For values of  $\theta$  greater than  $\theta_{opt}$ , soil CO<sub>2</sub> production decreases. We represented this by a bell shaped curve:

$$f_R(\theta) = \frac{0.9}{\sqrt{0.01\pi}} \exp\left(-\frac{(\theta-\theta_{opt})^2}{0.01}\right) \quad \text{and} \quad f_M(\theta) = \frac{1}{\sqrt{0.0081\pi}} \exp\left(-\frac{(\theta-\theta_{opt})^2}{0.0081}\right)$$

where  $f_R$  and  $f_M$  refers to the function used as part of the calculations for the soil CO<sub>2</sub> production from roots (R) and microbial (M) sources, and where  $\theta_{opt} = 0.3$ .

**Figure S1 Differences in daily  $R_{soil}$  from DETECT for the soil texture scenarios relative to the control scenario**

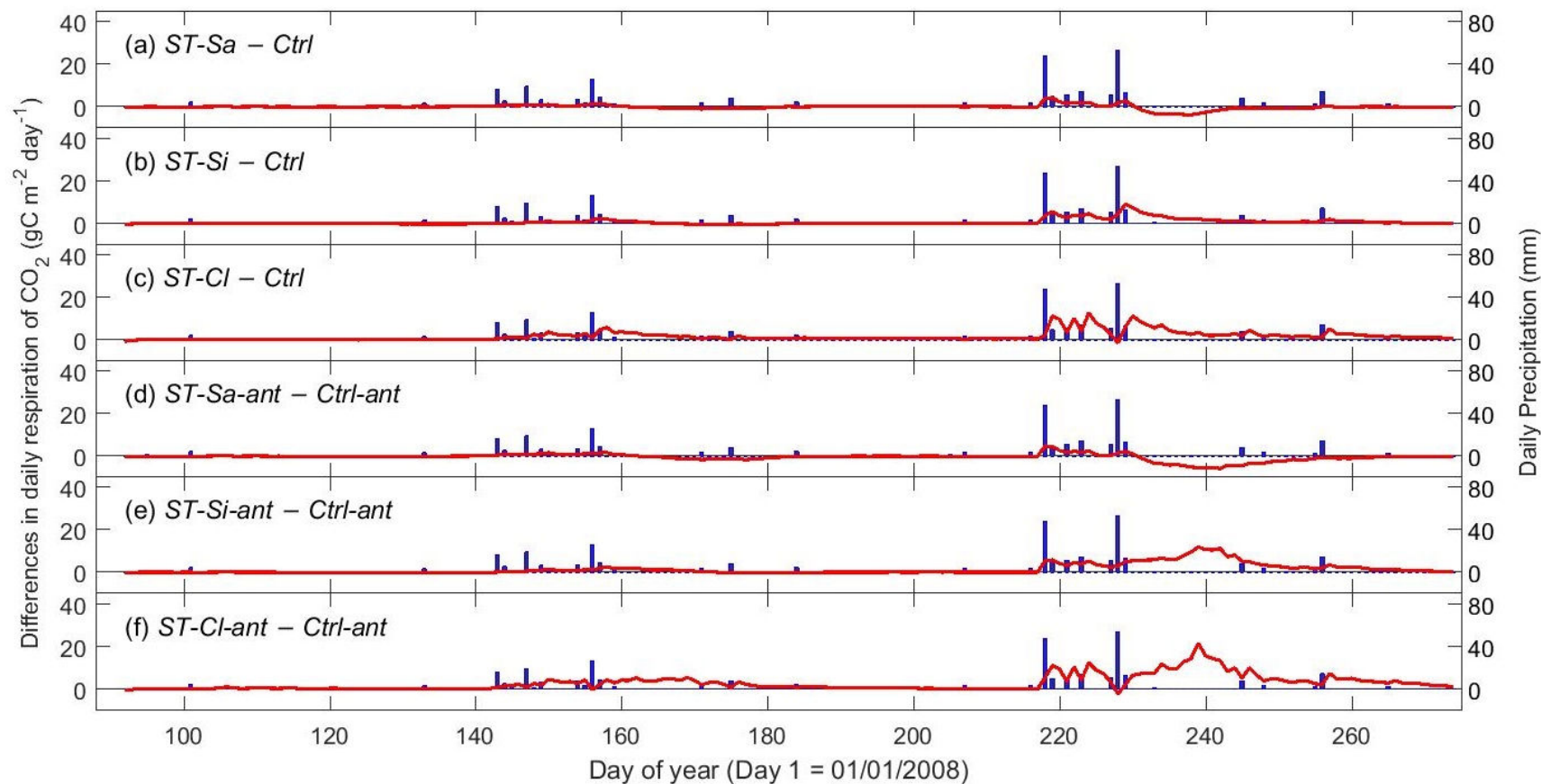


**Figure S1** Panels (a), (b), and (c) show the time-series of the daily soil respiration ( $R_{soil}$ ) from the non-steady state (DETECT) model for each soil texture scenario (*ST-Sa*, *ST-Si*, and *ST-CI*) minus  $R_{soil}$  predicted by the DETECT model for the control scenario (*Ctrl*); all scenarios do not incorporate antecedent effects. Panels (d), (e), and (f) show the same as the first three panels, respectively, except that the antecedent version of the DETECT model is used for the control and soil texture scenarios (*Ctrl-ant*, *ST-Sa-ant*, *ST-Si-ant*, and *ST-CI-ant*). See Table 2 in the main text for a description of the scenarios. Blue bars denote daily precipitation amounts.

**Figure S2 Differences in daily  $R_{soil}$  from DETECT for the precipitation scenarios relative to the control scenario**

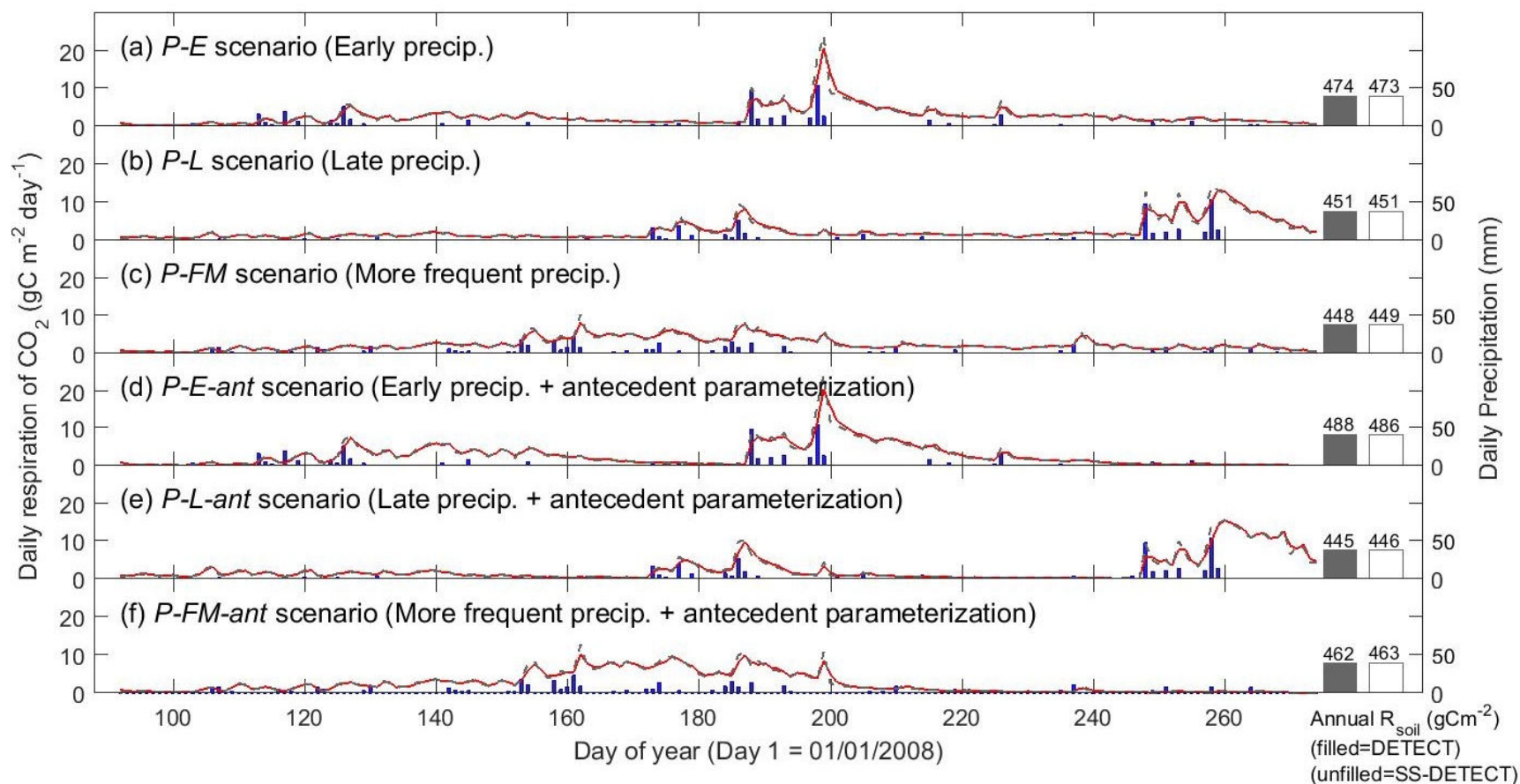


**Figure S2** Time-series of daily soil respiration ( $R_{soil}$ ) predicted from the non-steady-state (DETECT) and steady-state (SS-DETECT) models, for the precipitation scenarios using the non-antecedent (panels a, b, and c) and the antecedent (panels d, e, and f) parameterizations of the models. See Table 2 in the main text for a description of the scenarios. Blue bars denote daily precipitation amounts.

**Figure S3a Differences in daily  $R_{soil}$  from DETECT versus SS-DETECT for all non-antecedent scenarios**

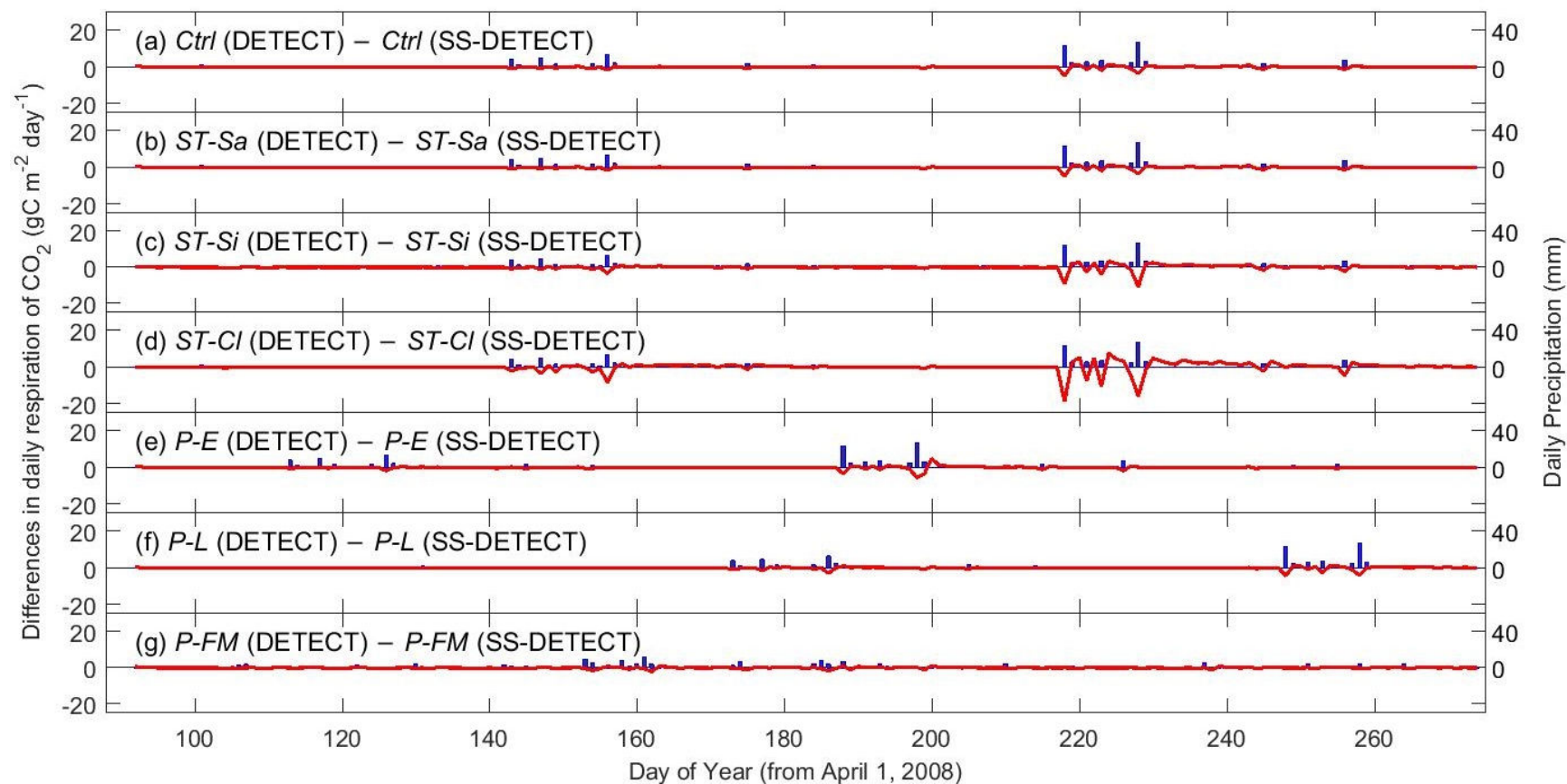


**Figure S3a** Time-series of difference in daily predicted soil respiration ( $R_{soil}$ ) between the non-steady-state (DETECT) and steady-state (SS-DETECT) models, for the non-antecedent scenarios (*Ctrl*, *ST-Sa*, *ST-Si*, *ST-CI*, *P-E*, *P-L* and *P-FM*). See Table 2 in the main text for a description of the scenarios. Blue bars denote daily precipitation amounts.

**Figure S3b Differences in daily  $R_{soil}$  from DETECT versus SS-DETECT for all antecedent scenarios**

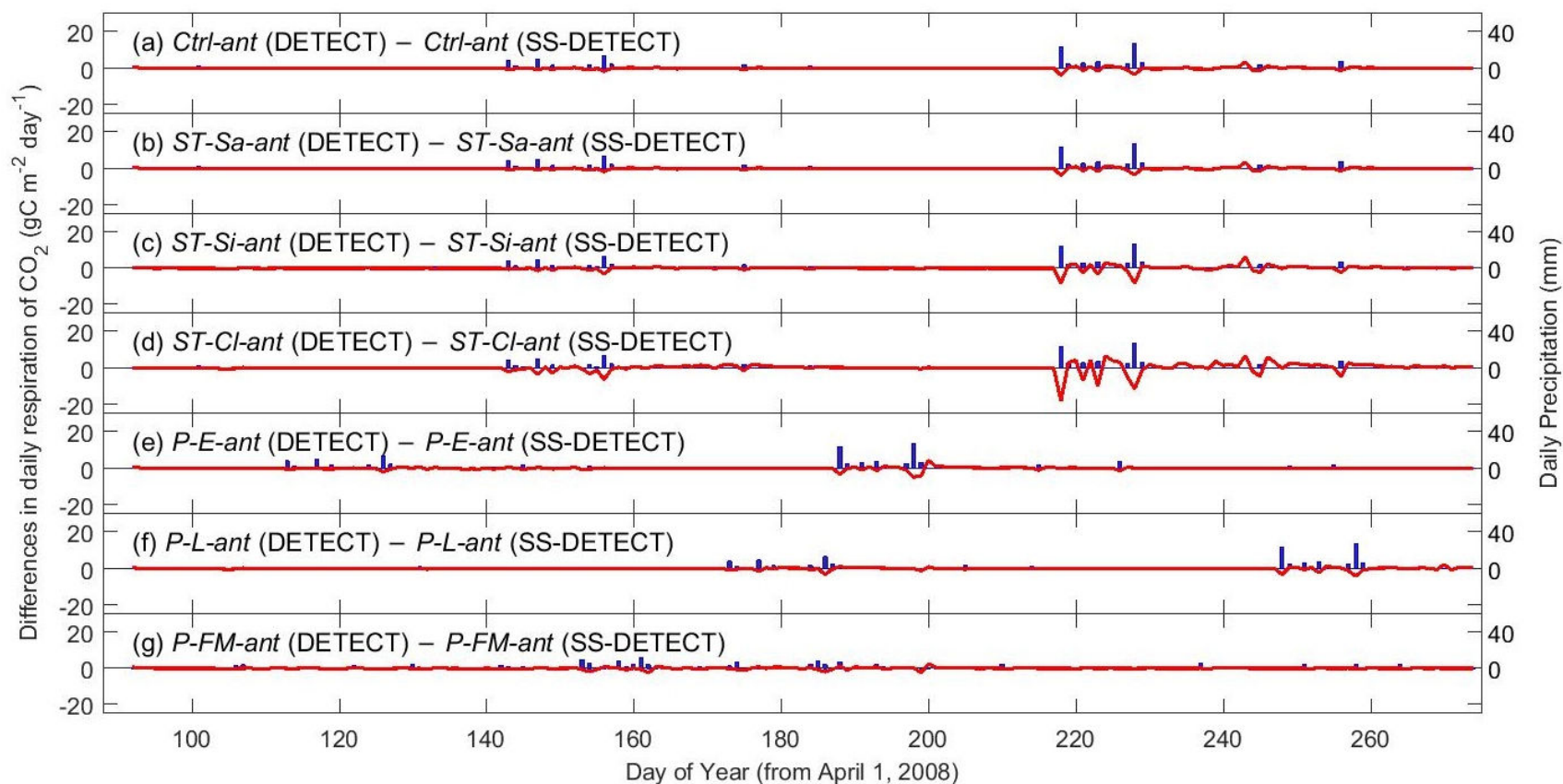


**Figure S3b** Time-series of difference in daily predicted soil respiration ( $R_{soil}$ ) between the non-steady-state (DETECT) and steady-state (SS-DETECT) models, for the antecedent scenarios (*Ctrl-ant*, *ST-Sa-ant*, *ST-Si-ant*, *ST-Cl-ant*, *P-E-ant*, *P-L-ant* and *P-FM-ant*). See Table 2 in the main text for a description of the scenarios. Blue bars denote daily precipitation amounts.

**Figure S4a Predicted versus observed soil CO<sub>2</sub> concentrations (*Ctrl* scenario)**

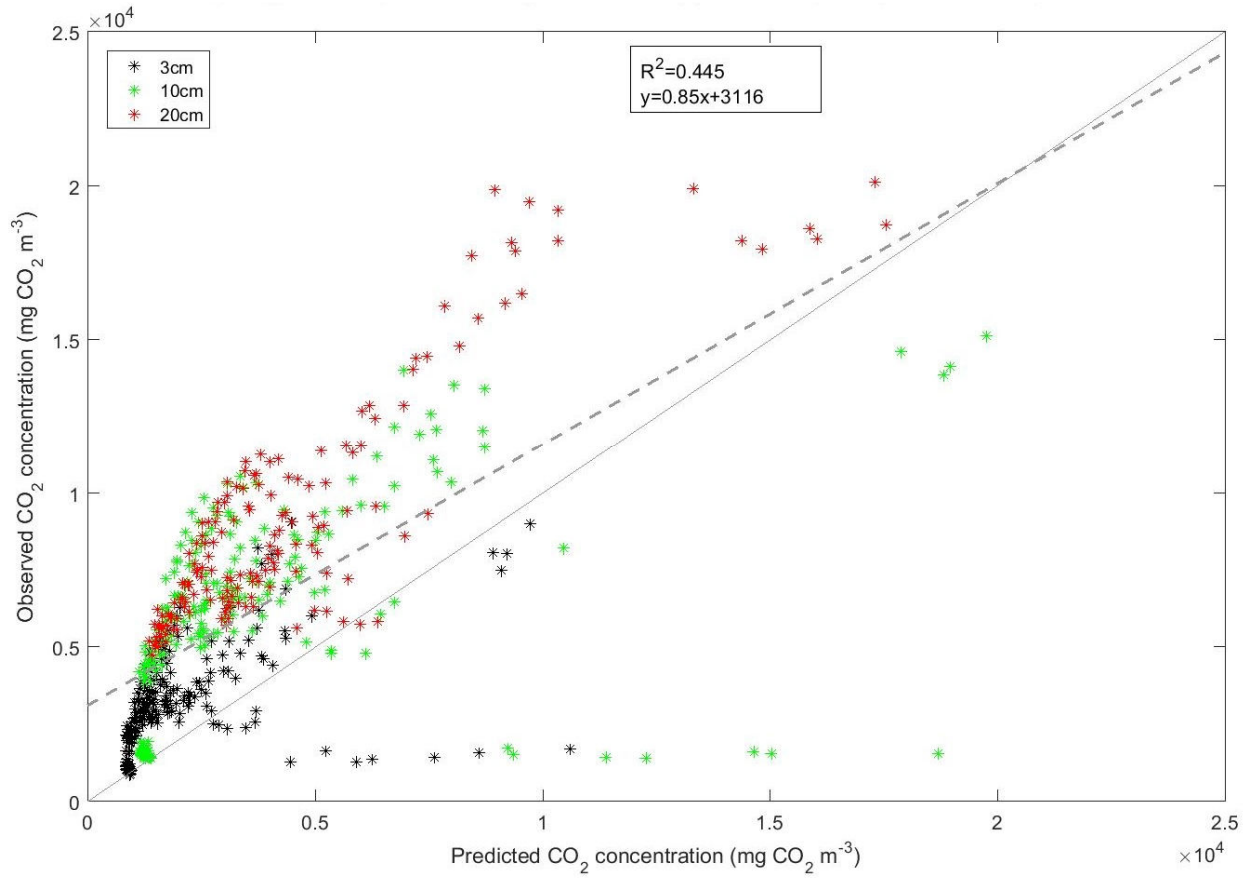


**Figure S4a** Predicted versus observed soil CO<sub>2</sub> concentrations, where the predictions are from the non-steady-state DETECT model used in the control (*Ctrl*) scenario, without antecedent effects. Observed soil CO<sub>2</sub> is based on soil gas probes installed at three depths (3, 10, and 20 cm) between April 1<sup>st</sup> and September 30<sup>th</sup>, 2008.

**Figure S4b Predicted versus observed soil CO<sub>2</sub> concentrations (*Ctrl-ant* scenario)**

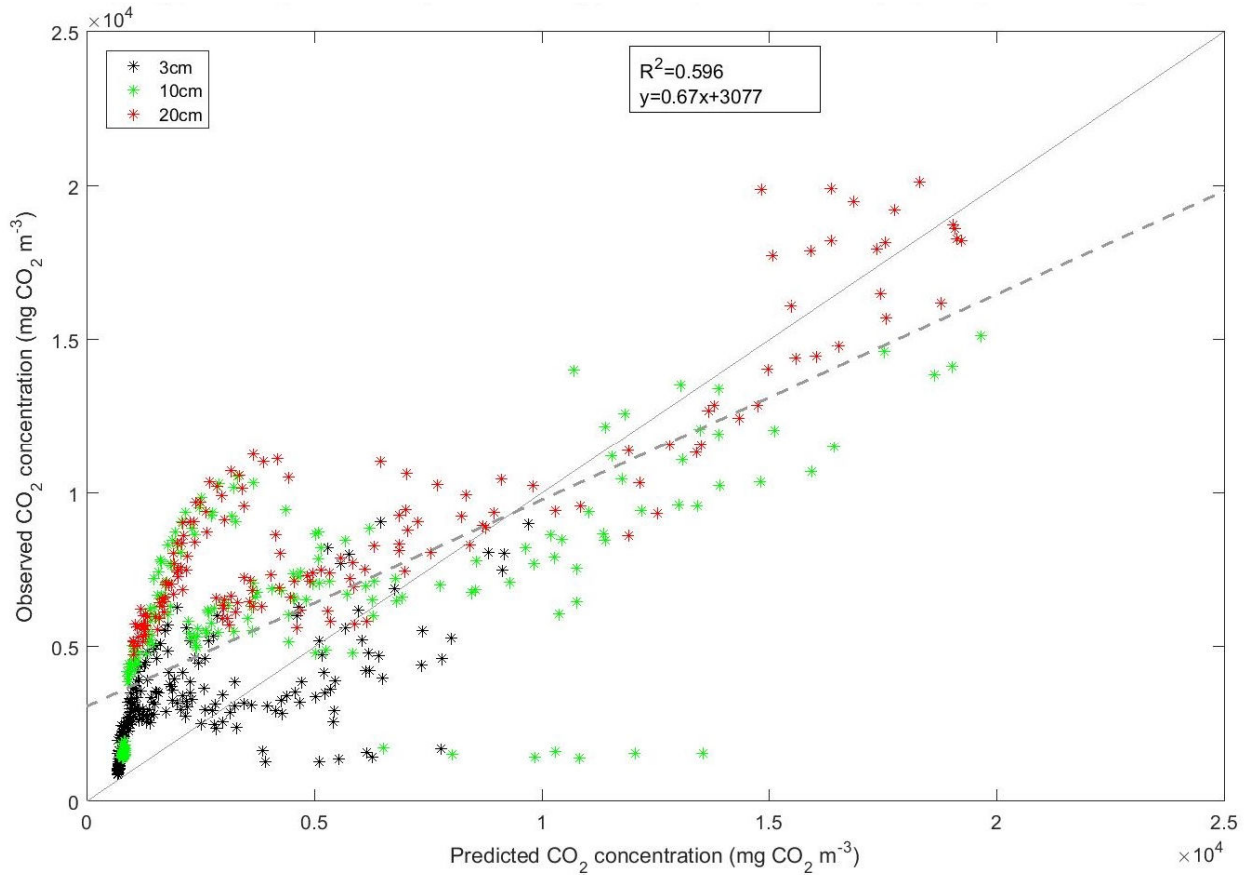


**Figure S4b** Predicted versus observed soil CO<sub>2</sub> concentrations, where the predictions are from the non-steady-state DETECT model used in the control scenario that includes antecedent soil water and temperature effects (*Ctrl-ant*). Observed soil CO<sub>2</sub> is based on soil gas probes installed at three depths (3, 10, and 20 cm) between April 1<sup>st</sup> and September 30<sup>th</sup>, 2008.

**Figure S5** Observed versus predicted values of belowground C

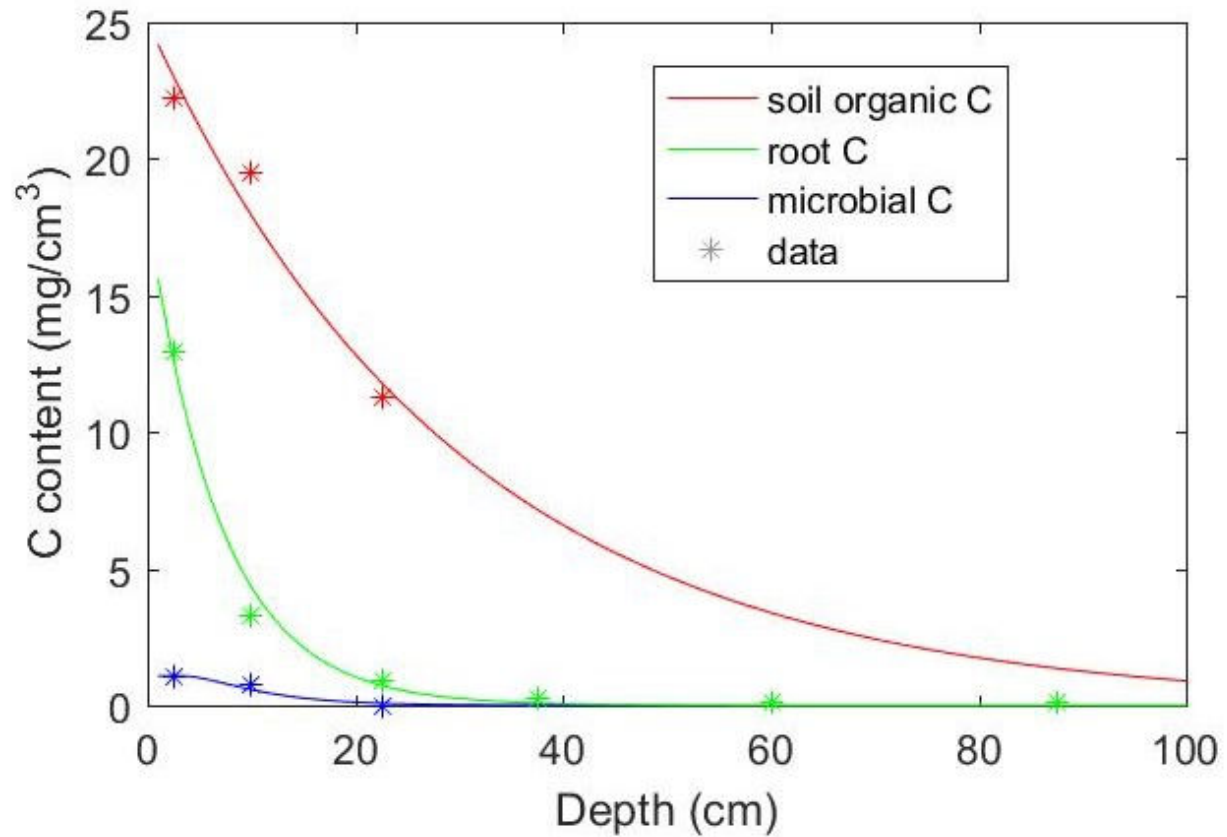


**Figure S5** Observed versus estimated soil organic, root, and microbial carbon (C) with depth. The lines represent functions that were fit to the data to inform  $C_{SOM}$ ,  $C_R$ , and  $C_{MIC}$ , respectively. See Section S1 for a description of the functions.

**Figure S6 Observed versus predicted values of soil CO<sub>2</sub>**

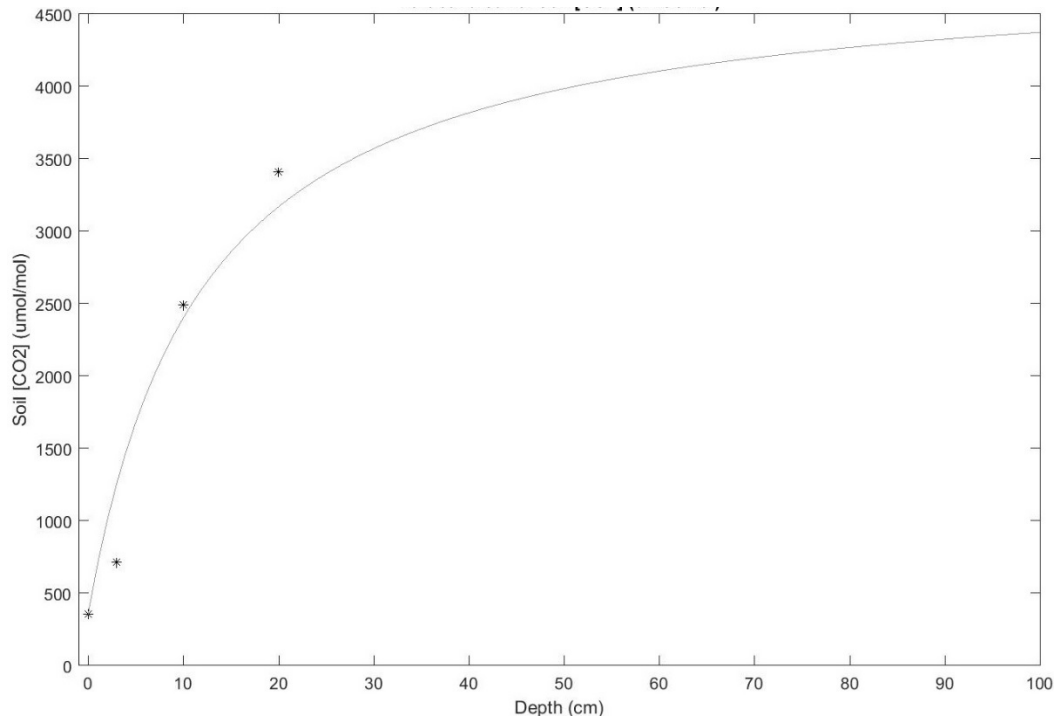


**Figure S6** Observed (stars) versus modelled (curve) soil CO<sub>2</sub> concentrations with depth. The data for each of the four depths (0, 3, 10, and 20 cm) are averages of measured soil CO<sub>2</sub> concentrations taken near the start of the 2007 growing season. See Section S2 for a description of the function, which was used to inform the initial conditions,  $c(z, 0)$ .

**Figure S7 Observed versus predicted values of microbial respiration**

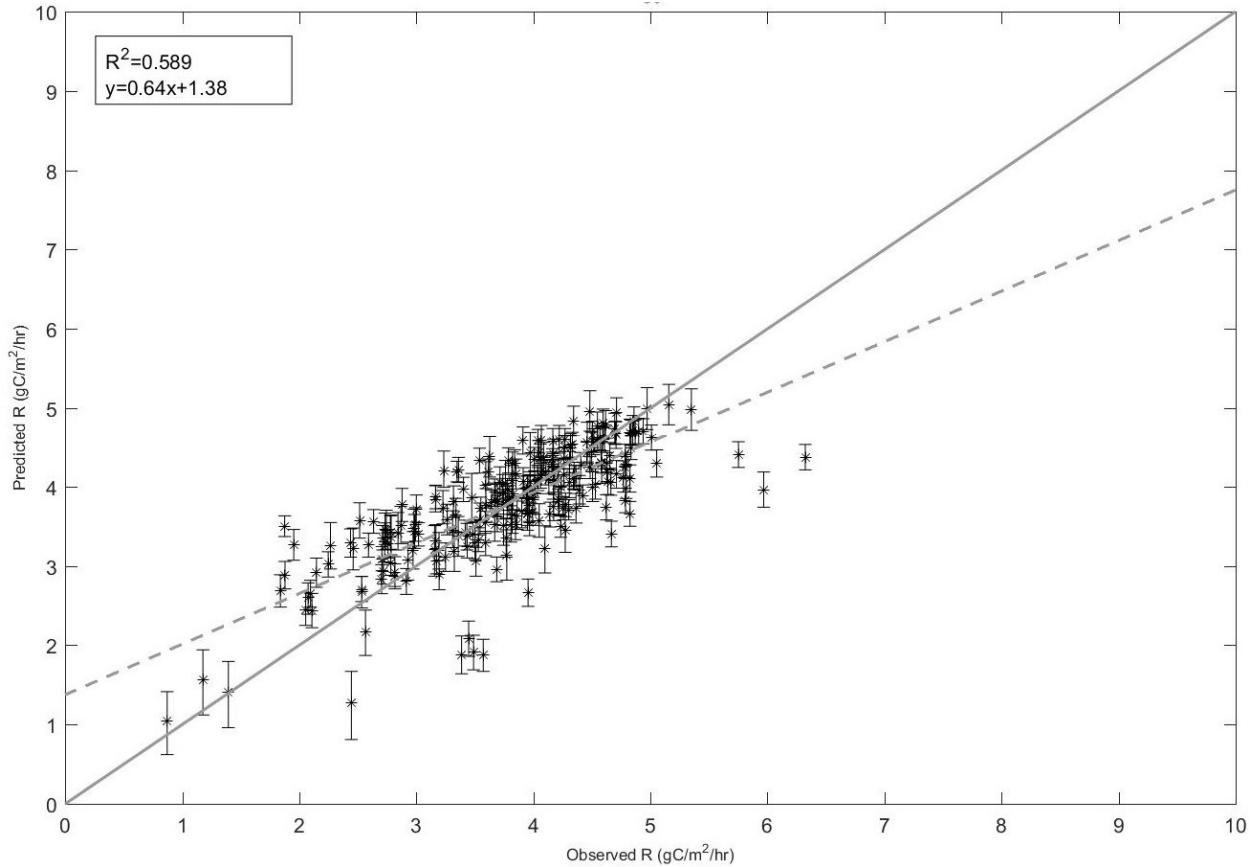


**Figure S7** Observed surface-soil respiration derived from microbes (heterotrophs) from the PHACE experiment—based on ecosystem respiration measurements made on non-vegetated plots—versus predicted surface soil respiration due to microbes as informed by the microbial source term submodel (Eqn 5), but without the microbial C or CUE terms. The data were obtained by measuring the change in CO<sub>2</sub> concentration using a trace gas chamber, from a portion of each plot where herbicide was applied to remove all plant matter at the beginning of 2008. We assumed that during the first year after application of the herbicide, the microbes in the soil were respiring at the same rate as before the application. See Dijkstra et al. (2013) and Ogle et al. (2016) for details about the microbial respiration measurements and application of the herbicide.

**Figure S8 Different formulations of the soil water content functions used in DETECT.**

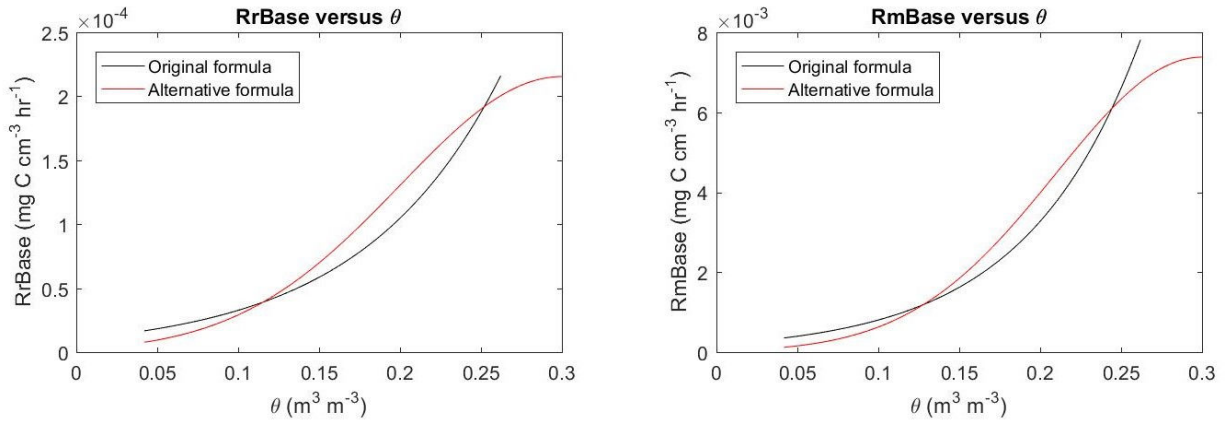


**Figure S8** The panel on the left of this figure shows the graphical representation of the equation that models RrBase as a function of  $\theta$ , where RrBase is the base rate of Rr (production of root  $\text{CO}_2$ ) and  $\theta$  is the soil water content. This equation is one of the equations used to calculate microbial  $\text{CO}_2$  production, where the other equations use this RrBase value to allow production to vary according the specific temperature and microbial C content of a particular depth. Here we show two options for modelling RrBase as a function of  $\theta$ : (1) the exponential type function used in this analysis (see equation 4a of the paper); (2) an alternative to equation 4a, where RrBase increases as  $\theta$  increases, but only up until a certain point given by  $\theta_{\text{opt}}$ ; for values of  $\theta$  higher than  $\theta_{\text{opt}}$ , RrBase decreases. For the Wyoming field site that we use to make measurements,  $\theta$  never got high enough that resulted in ecosystem respiration  $\text{CO}_2$  rates to decrease. Hence, the graphical representation of this alternative RrBase function shows RrBase increasing for values of  $\theta$  up to  $\theta_{\text{opt}}$ . The description of the panel on the right of this figure is exactly the same as the left panel except that the y-axis shows RmBase (microbial production of  $\text{CO}_2$ ) instead of RrBase.  $\theta_{\text{opt}} = 0.3$  (see Section S4) was chosen such that the black and red lines above matched as closely as possible, but we emphasize that the equation in Section S4 is just one alternative to equation (4a) in order to demonstrate the possibility of having a bell-shaped curve as the respiration versus  $\theta$  function. There may be other formulations and other parameterizations that would be suitable also.

**Figure S9** Time series of predicted  $R_{soil}$  (i.e. similar to figure 2) but using the alternative soil water content function

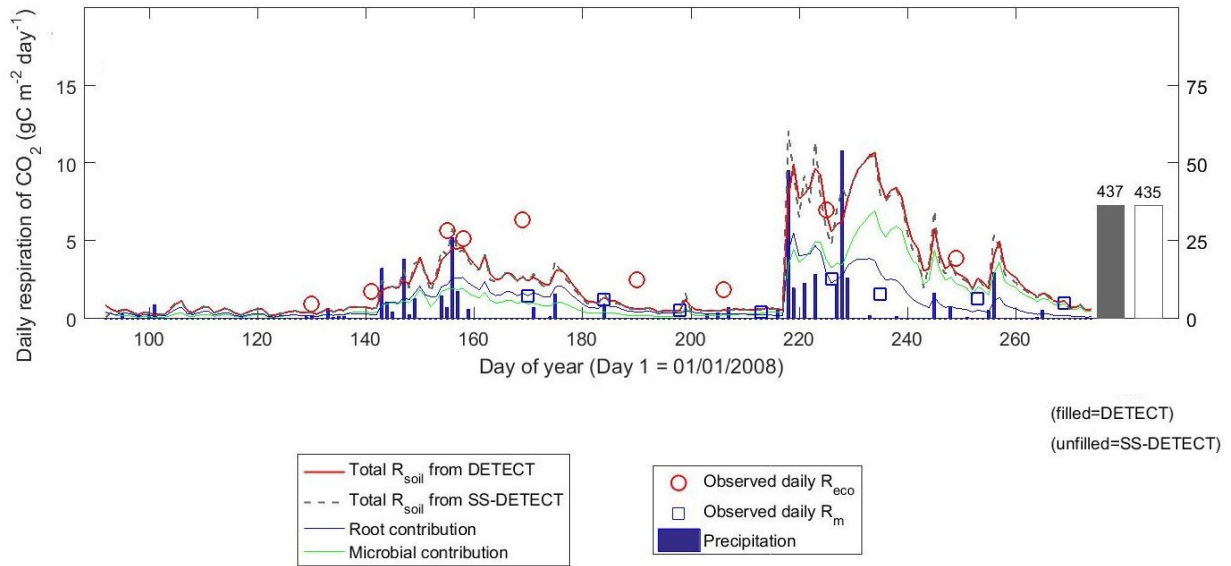


**Figure S9** The description for this figure is exactly the same as that of figure 2a, except that the function used to simulate the production of soil  $CO_2$  from root and microbial sources is a bell shaped curve (see Section S4) rather than an exponential function as used for the results of this analysis (see equation 4a of manuscript).

**Figure S10 Modelled values of production versus soil water content for different soil depths**

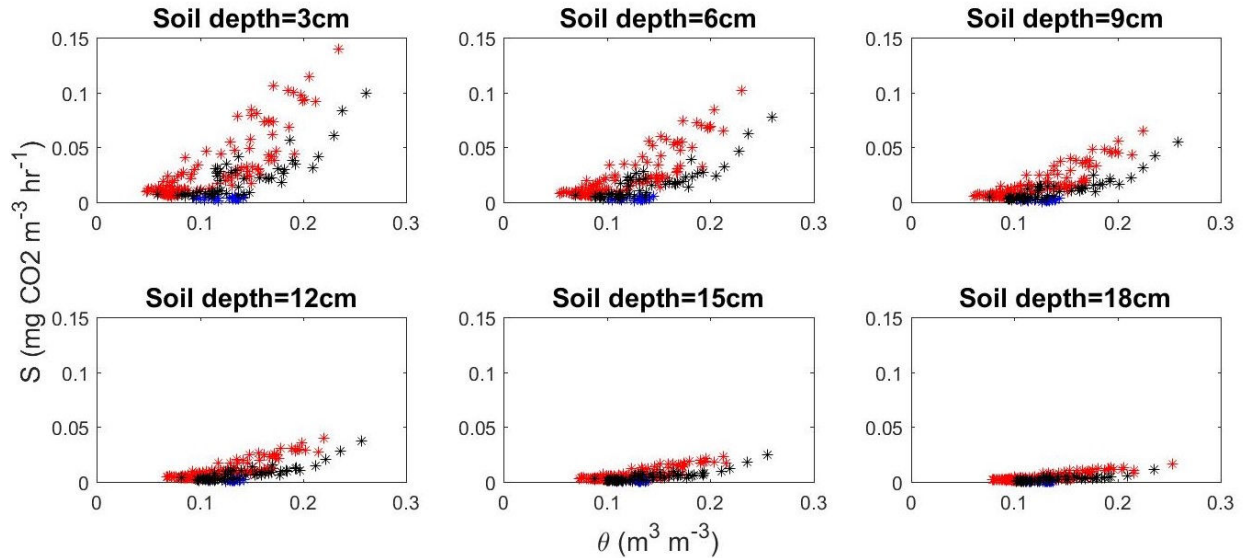


**Figure S10** Graphical representation of total production of CO<sub>2</sub> from root and microbial sources ( $S$ , mg CO<sub>2</sub> m<sup>-3</sup> hr<sup>-1</sup>) as modelled by DETECT versus soil water content ( $\theta$ , m<sup>3</sup> m<sup>-3</sup>) at different soil depths. The different colors of the points represent different soil temperatures: above 12°C (red), between 4°C and 12°C (black), and below 4°C (blue).

## References

- Carrillo, Y., Dijkstra, F. A., LeCain, D., Morgan, J. A., Blumenthal, D., Waldron, S., and Pendall, E.: Disentangling root responses to climate change in a semiarid grassland, *Oecologia*, 2014. 1-13, 2014.
- Dijkstra, F. A., Carrillo, Y., Pendall, E., and Morgan, J. A.: Rhizosphere priming: a nutrient perspective, *Frontiers in microbiology*, 4, 2013.
- Ogle, K., Ryan, E., Dijkstra, F. A., and Pendall, E.: Quantifying and reducing uncertainties in estimated soil CO<sub>2</sub> fluxes with hierarchical data-model integration, *Journal of Geophysical Research: Biogeosciences*, 2016. 2016.
- Zelikova, T. J., Williams, D. G., Hoenigman, R., Blumenthal, D. M., Morgan, J. A., and Pendall, E.: Seasonality of soil moisture mediates responses of ecosystem phenology to elevated CO<sub>2</sub> and warming in a semi-arid grassland, *Journal of Ecology*, 2015. 2015.